Electronic Supplementary Material (ESI) for Energy & Environmental Science.
This journal is © The Royal Society of Chemistry 2015

Supplementary Information For:

An Electrochemical Engineering Assessment of the Operational Conditions and Constraints for Solar-Driven Water-Splitting Systems at Near-Neutral pH

Meenesh R. Singh, Kimberly Papadantonakis, Chengxiang Xiang*, and Nathan S. Lewis*

1. MODELING

1.1 Physical properties

Table 1 lists the kinetic parameters assumed for the simplified, one-dimensional model of a photoelectrochemical cell in which the hydrogen-evolution reaction (HER) is catalyzed by platinum at the cathode and the oxygen-evolution reaction (OER) is catalyzed by iridium oxide at the anode.

Table 1: List of kinetic parameters for OER and HER

Parameter	Description	Values
i_0 (OER)	OER exchange current density	1.4×10^{-3} A m^{-2}
α_a (OER)	OER anodic transfer coefficient	1
α_c (OER)	OER cathodic transfer coefficient	0.1
i_0 (HER)	HER exchange current density	10 A m^{-2}
α_a (HER)	HER anodic transfer coefficient	2.57
α_c (HER)	HER cathodic transfer coefficient	2.57
E_0	Equilibrium potential	1.229 V
T	Reaction temperature	298 K

Table 2 lists the diffusion coefficients assumed for the transport of ionic and neutral species in the electrolyte.

Table 2: Ionic diffusion coefficients in water at 298 K

Species	**Diffusion Coefficients** $\left(\times 10^9\ \mathrm{m^2\ s^{-1}}\right)$	**Modified Diffusion Coefficients*** $\left(\times 10^9\ \mathrm{m^2\ s^{-1}}\right)$
H^+	9.311	63.911
K^+	1.957	56.557
HPO_4^{2-}	0.439	55.039
SO_4^{2-}	1.065	55.665
$H_2PO_4^-$	0.879	55.479
HSO_4^-	1.331	55.931
OH^-	5.273	59.873
Cl^-	2.032	56.632
A^-	1.000	55.600
HA	1.500	56.100

* Modified diffusion coefficients were obtained by adding bubble-induced momentum $h_{\mathrm{el}} \times v_{\mathrm{terminal}}$ to the diffusion coefficients of species. Here h_{el} is the height of the electrode and v_{terminal} is the terminal velocity of bubbles. The value of bubble-induced momentum is $54.6 \times 10^{-9}\ \mathrm{m^2 s^{-1}}$.

2. ANALYSIS OF THE DISTRIBUTION OF IONIC SPECIES IN A STAGNANT ELECTROLYTE BUFFERED AT NEUTRAL pH

Figure S1 shows an analysis of the partial current densities and the concentration distribution of different ionic species in the plateau region below the limiting current density in a pH=7 electrolyte. Three distinctive physical zones, in which the major ionic species that carry the current density are significantly distinctive, can be present between the anode and the cathode: the cathode zone, the anode zone and the bulk zone. At low applied voltages (<1.65 V), the current density in the electrolyte was primarily carried by the conjugate base, and the partial current density distributions of different ionic species were very similar in all three zones. As the current density increased, the concentration of the conjugate base started to decrease and the proton concentration started to increase in the anode region. In the quasi-plateau region (1.7 V to 1.8 V), the concentration and the partial current density of the conjugated base decreased rapidly

(Figure S1b) and the pH gradients at the anode zone increased significantly (Figure S1c). At the end of the quasi-plateau region, the conjugated base was depleted in the anode zone and the current density was carried by the produced protons. As the applied voltage increased above 1.9 V, the current-voltage relation approached the limiting current density, in which the depletion region of the conjugated base at the anode zone started to expand and the conjugated acid started to deplete in the cathode zone (Figure S1c). As the operating current density approached the limiting current density, three different zones developed in the electrolyte: an acidic layer near the anode with a pH = 2; an alkaline layer near the cathode with a pH = 10; and a buffered zone of neutral pH between the acidic and alkaline layers.

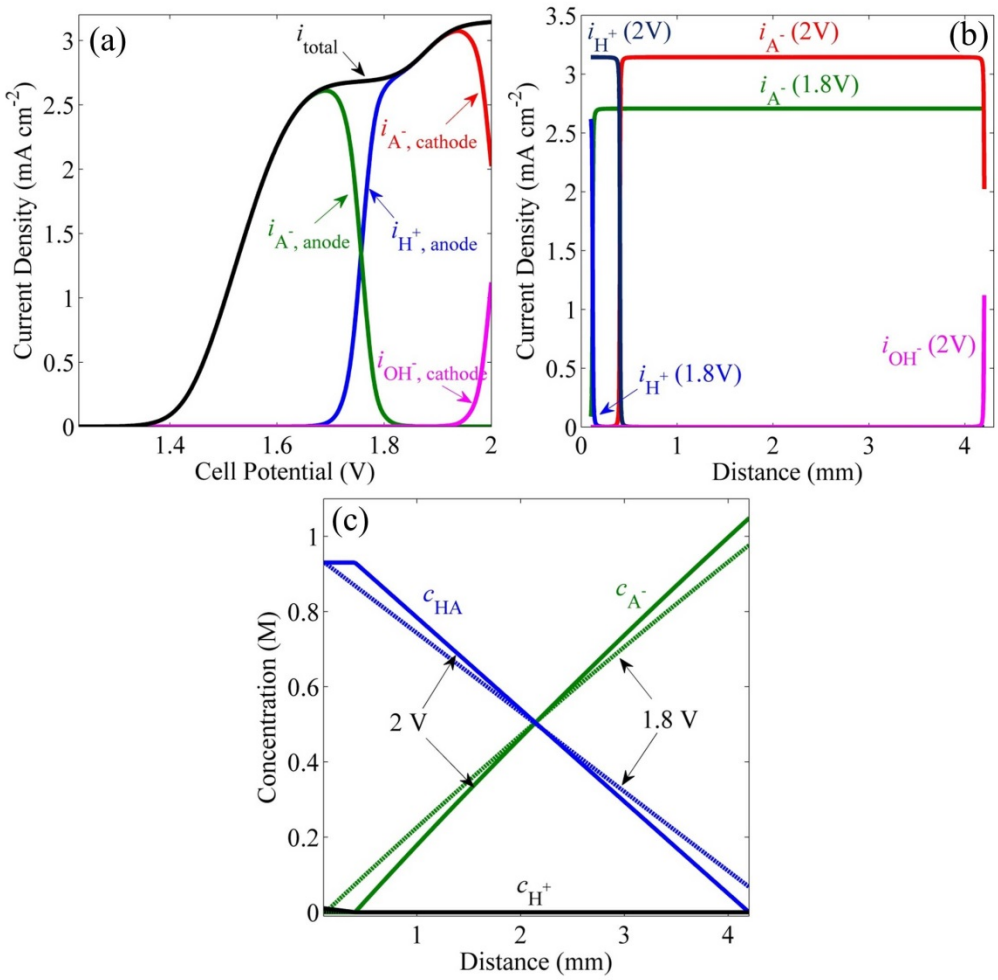

Figure S1. (a) Analysis of the voltage-dependent distribution of current-carrying species in a cell buffered at pH = 7 and containing a supporting electrolyte. The current was carried by the conjugate base (A^-), protons (H^+), and hydroxide ions (OH^-) at anode and cathode. (b) Partial

current density as a function of distance from the anode for applied voltages of 1.8 V and 2.0 V (corresponding to the two plateau regions in the J-V plot, the cathode was located at $x = 4$ mm). (c) Concentration of buffer species in solution as a function of distance for applied potentials of 1.8 V (dotted lines) and 2.0 V (solid lines). The conjugate acid of the buffer saturated at the anode and depleted at the cathode in the potential range of 1.8–2.0 V.

3. STAGNANT ELECTROLYTES BUFFERED AT pH NOT EQUAL TO pK_a

Figure S2a shows the limiting current density for cells containing electrolytes buffered to pH = 3 using buffers with a range of pK_a values (specifically by varying the concentration ratios of the conjugate acid and base). The limiting current density increased with the pK_a of the buffer until the pK_a of the buffer was much greater than the pH of the solution ($pK_a \sim 5$). Although the limiting current density increased with the pK_a of the buffer, such monotonic behavior of the current density with pK_a was only observed for high (>1.7 V) potentials. A fundamentally different phenomenon was apparent at lower potentials, as shown in Figure 6b. At potentials lower than those needed to reach the limiting current densities, the current density was greatest for the buffer with pK_a = pH (Figure S2b).

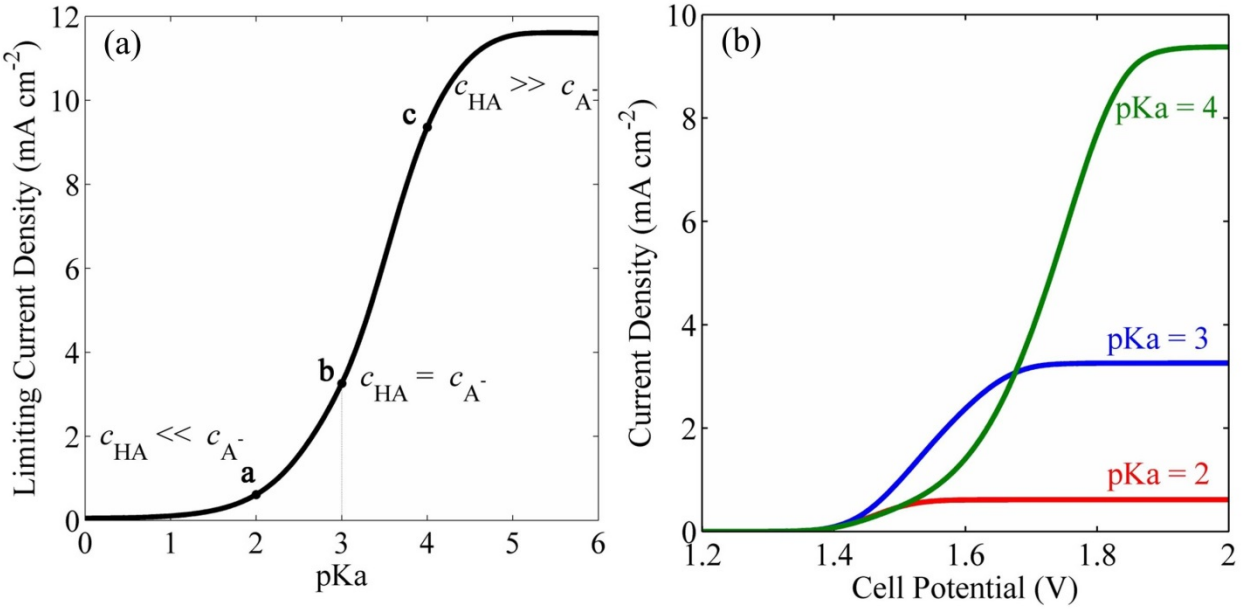

Figure S2. (a) Limiting current density as a function of the pK_a of the buffer species for a stagnant electrolyte buffered at pH = 3 using 1 M buffer. (b) Current-density versus behavior for a cell containing an electrolyte buffered at pH = 3 using 1 M of a buffer with $pK_a = 2$ (< pH), $pK_a = 3$ (= pH), and $pK_a = 4$ (> pH).

4. PARTIAL CURRENT-DENSITY DISTRIBUTIONS FOR MEMBRANE-CONTAINING CELLS WITH STAGNANT BUFFERED ELECTROLYTES

Figures S3a-b show the current density versus cell potential for a stagnant cell containing either a neutrally charged or a negatively charge conjugated acid. In the case of the negatively charged conjugated acid (hydrogen phosphate ion), the net current density is smaller than that for the neutrally charged conjugated acid. Figure S3c shows the partial current density distribution due to protons, hydroxide ions and conjugate base at an applied potential of 2 V (corresponding to the limiting current density) as a function of distance from the anode, for a cell with a stagnant electrolyte buffered at neutral pH using a buffer with an uncharged conjugate-acid species. In the CEM case, the partial current density carried by protons spanned the anolyte and the CEM regions, and acidification of the CEM produced a higher limiting current density than for the AEM and membrane-free systems. For a negatively charged conjugate-acid species, the current density decreased due to the negative partial current density carried by the charged conjugate-acid species (Figure S3d). Alternatively, the polarization losses were higher in the phosphate buffer than in the neutrally charged buffer, because the concentration gradient of the negatively charged conjugate acid was opposed to the electric field. The partial current densities carried by conjugate base were close to those carried by the conjugate base in the neutral conjugate-acid case. Figure S3d also shows that the partial current-density distribution of protons could not cross the CEM and therefore the net current density was limited by the diffusion of anions through the CEM.

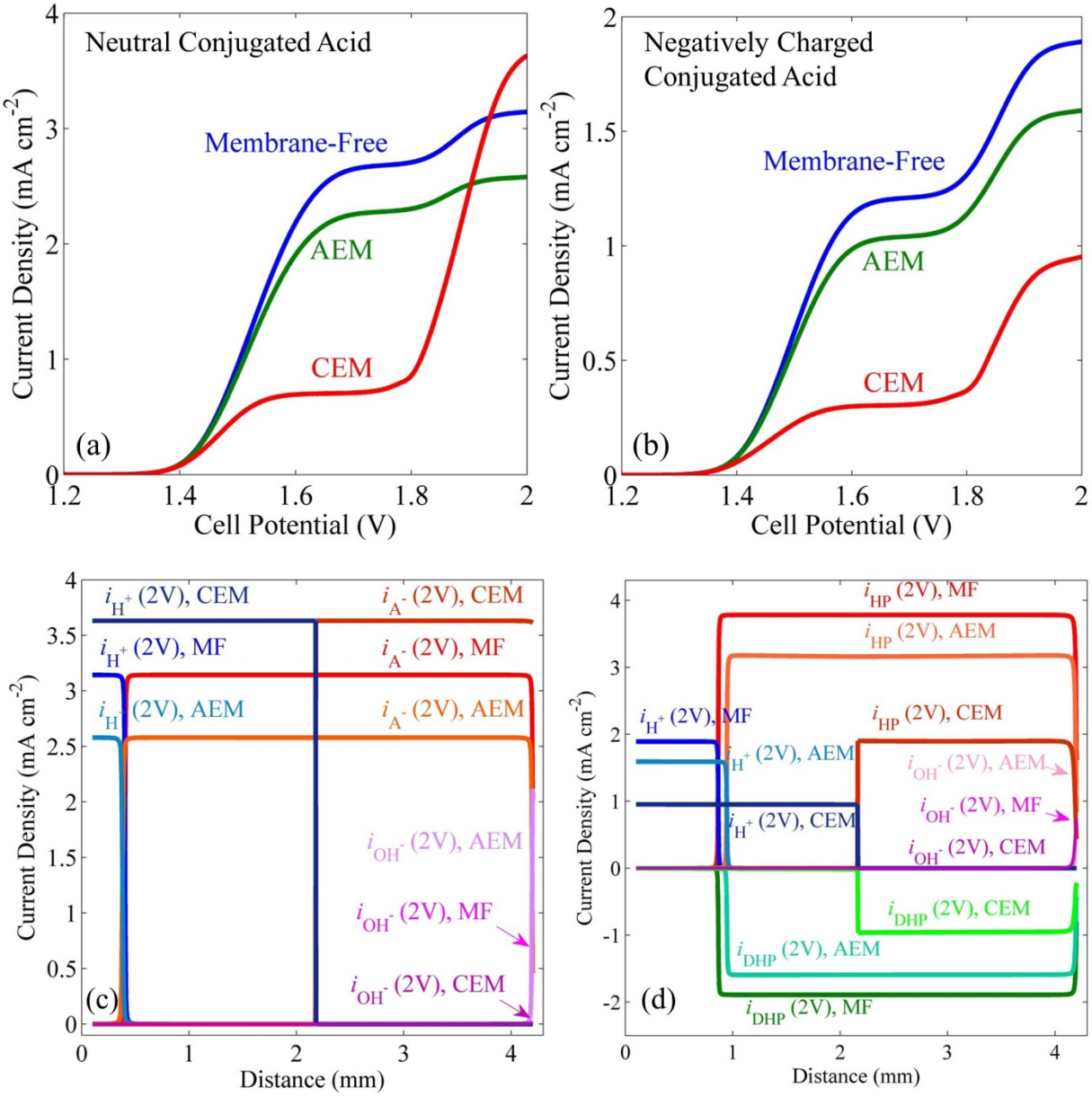

Figure S3. Current-density versus voltage behavior of a cell containing a stagnant electrolyte buffered at neutral pH and employing an anion-exchange membrane (AEM), cation-exchange membrane (CEM), or no membrane to separate the gaseous products of electrolysis. The conjugate acid of the buffer in (a) was a neutral species, whereas the conjugate acid of the buffer in (b) was a negatively charged species as in the phosphate buffer system. (c) and (d) show partial current density at an applied potential of 2 V as a function of distance for the cases shown in a & b, respectively. (c) For a buffer with a neutral conjugate-acid species, the current was carried by protons (H^+), hydroxide ions (OH^-), and the conjugate base (A^-). (d) For a buffer with a negatively charged conjugate acid (such as in the phosphate buffer system), the current was carried by protons (H^+), hydroxide ions (OH^-), and the conjugate base (DHP: HPO_4^{2-}). The negative current is due to diffusion of conjugated acid (HP: $H_2PO_4^-$). MF, AEM and CEM indicate membrane-free, anion-exchange and cation-exchange membrane cases, respectively.

5. EFFECTS OF BUFFER CONCENTRATION AND BOUNDARY LAYER THICKNESS ON POLARIZATION LOSSES

Figure S4a shows the polarization losses at an operating current density of 10 mA cm^{-2} (corresponding to a solar-driven water-splitting system operating at a solar-to-hydrogen efficiency of 12.3%) for membrane-free cells that contained stagnant buffered electrolytes, relative to the behavior of a cell that contained a strongly acidic electrolyte at pH = 0. At low buffer capacity (< 1 M), the polarization losses increased rapidly with pH, and the limiting current density for the electrolyte with pH > 0.9 was less than 10 mA cm^{-2}. Thus, at buffer capacities < 1 M and in the absence of convective flow, an operating current density of 10 mA cm^{-2} was not attainable for the modelled system at any pH > 0.9, no matter how much potential was applied. Increasing the buffer capacity to 3.5 M significantly reduced the polarization losses, to a value < 200 mV for all pH values, and also limited the pH gradient at the electrodes relative to cases that had a lower buffer concentration. For example, the pH values at the anode and cathode of a cell using an electrolyte buffered at pH = 7 by 3.5 M buffer were 5.7 and 8.3, respectively. For example, a phosphate buffer of 3.5 M capacity would need 1.75 M of monopotassium phosphate and 1.75 M of dipotassium phosphate. The solubility of monopotassium phosphate is ~ 1.6 M and dipotassium phosphate is ~ 8.6 M. Even if a 3.5 M phosphate buffer could be prepared (for example using higher temperatures), the buffer capacity of the solution would be limited by crystallization of the buffer due to electrodialysis of the solution. An alternative to preparing an aqueous 3.5 M buffer is to use an ionic liquid buffer such as choline monohydrogen phosphate and choline dihydrogen phosphate, which has a higher buffer capacity, of up to 5 M.

Figure S4b shows the relative polarization losses as a function of pH for membrane-free cells that contained 1 M buffer but that utilized three different boundary layer thicknesses. The polarization losses decreased with a decreased boundary layer thickness for a given electrolyte

pH. Although a boundary layer thickness of 8 mm or 4 mm caused the buffer to deplete for electrolytes of pH < 1, an order-of-magnitude decrease in the boundary layer thickness reduced the polarization losses to < 45 mV, even for an electrolyte buffered at near-neutral pH.

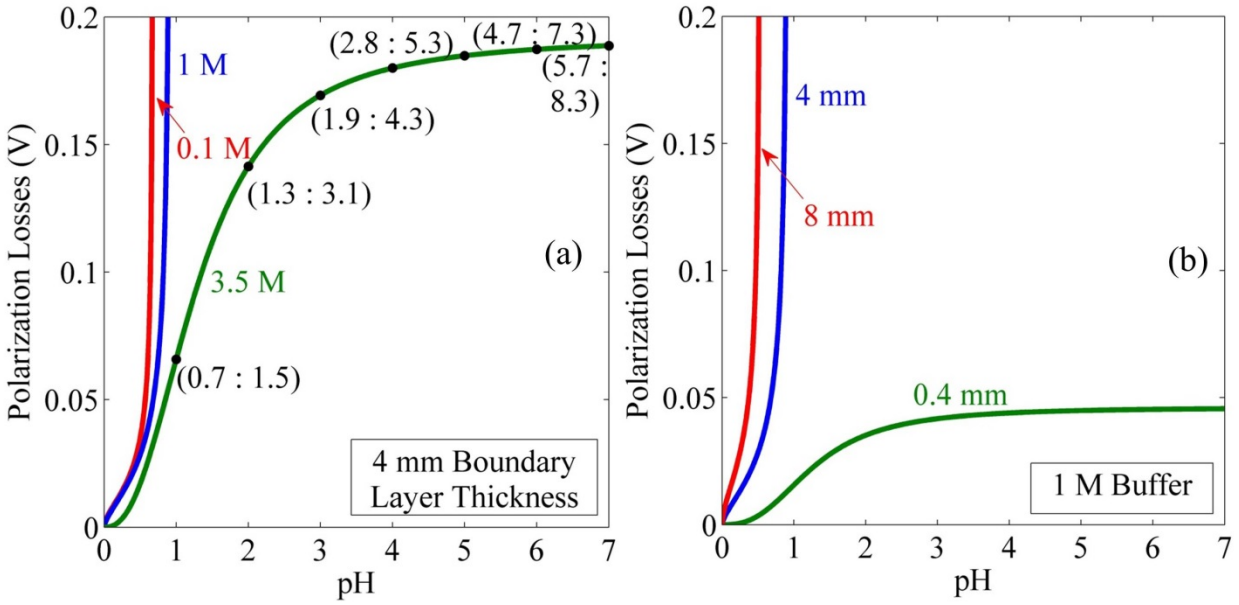

Figure S4. (a) Polarization losses at an operating current density of 10 mA cm^{-2} for membrane-free cells containing stagnant buffered electrolytes relative to a cell containing a strongly acidic electrolyte at pH = 0. The pH values at the anode and cathode (which deviated from the bulk values) are given in the parentheses (pH at anode : pH at cathode). (b) Relative polarization losses at an operating current density of 10 mA cm^{-2} as a function of pH for three different boundary layer thicknesses for a cell with a buffer capacity of 1M.